Journal of Materials Chemistry B

Accepted Manuscript

ROYAL SOCIETY OF CHEMISTRY

www.rsc.org/materialsB

Graphic Abstract

Gypsum-introduced, CaO-rich dicalcium silicate-based cements exhibit multifucntional physiochemical and biological properties and meet some challenging criteria in root canal therapy.

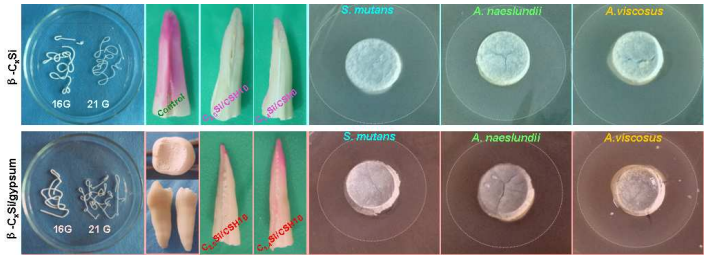

Cite this: DOI: 10.1039/c0xx00000x

www.rsc.org/xxxxxx

Full Paper

Rational design and fabrication of a β-dicalcium silicate-based multifunctional cement potential for root canal filling treatment

Xianyan Yang, [a]† Min Liu, *[b]† Yu Zhao, [b] Hongyu Jia,[b] Sanzhong Xu,[c] Xigong Li,[c] Xiaoyi Chen,[a] Feng Zhang,[d] Changyou Gao,[a] Zhongru Gou*[a]

Received (in XXX, XXX) Xth XXXXXXXXX 20XX, Accepted Xth XXXXXXXXX 20XX
DOI: 10.1039/b000000x

The integration of physicochemical and biological performances in root canal treatment represents a challenge for long-time antileakage, antibacteria, and even inducing periradicular cementum/bone tissue regeneration. The objective of this work is to develop a β-Ca_2SiO_3 (β-C_2Si)-based cement as new root canal filler with good antibacterial ability, sealability and bioactivity. The β-C_2Si powders with controllable free CaO content were prepared by regulating the calcium/silicate molar ratio in reaction medium. It was demonstrated that a composite paste with 10−30 wt% α-gypsum at a liquid-to-powder ratio of 0.6 ml g^{-1} remained injectable for 12 min, and significant pH rise during setting. Notably, the hydraulic cements with high free CaO contents exhibited bacterialcidal or bacteriostatic properties against three bacterial strains, streptococci mutans, actinomyces naeslundii, and actinomyces viscosus, which were demonstrated by the agar diffusion method. Also, the injected paste in root canal ex vivo showed extremely low microleakage of Rhodamine B but good apatite-mineralization response. Therefore, these intrinsic antibacterial activity, bioactivity, injectability and tight adaption to root canal sealability make the β-C_2Si/α-gypsum composites preferential candidates for application in endodontics, such as root root-end filling, pulp capping therapy, microleakage prevention, as well as inducing hard tissue regeneration.

Introduction

"Save a Tooth" is a key phrase in dentistry today. Root canal therapy is a commonly used method to treat reversible pulpitis and periradicular inflammation. The success of such treatment depends, among other goals, on the best possible debridement, sterilization and then full closure of root canal system. Conversely, inadequate obturation risks bacteria-laden saliva and tissue fluid penetration to the root apex, leading to periradicular chronic inflammation, which is one of the most important concerns for dentists, patients and public healthcare system [1].

The primary root canal treatment is associated with the eradication of microbes (if present) from the root-canal system. Calcium hydroxide (CH)-distilled water paste is widely used as a temporary intracanal cleaning medicament to debride the micro-organisms because of its antimicrobial activity[2]. CH paste also releases calcium ions and accompanies with pH rise, which may enhance the potential of mineralized tissue formation and inhibit osteoclastic activity[3,4]. However, the pure CH paste should be removed prior to permanent canal filling due to some known disadvantages, such as nonadherence to dentine, dissolution in tissue fluid, and poor sealing properties[5].

The filling materials that can provide permanent apical sealing and the ability to stimulate diverse diseased periradicular tissue (i.e., periodontium, alveolar bone and root cementum) healing or regeneration are of special significance for the success of root canal treatment. Numerous materials have historically been used for root canal filling, such as zinc oxide-eugenol cement, composite resin and glass ionomer cement. However, these materials have cytotoxic potential, or may cause severe inflammatory reactions if they gain access into periapical area[6,7].

Mineral trioxide aggregate (MTA), as a derivative of Portland cement, has developed as promising filler for root-end sealing, perforation repair and vital pulp therapy[8-10]. MTA is a mixture of linker including β-dicalcium silicate (β-C_2Si), tricalcium silicate (C_3Si), calcium aluminate, calcium sulfate and other impurities. The later, added either deliberately or accidentally, would alter both hydration and final hydrated cement properties. The early studies have shown that MTA prevents microleakage, is biocompatible, and promotes regeneration of original tissues when it is placed in contact with the dental pulp or periradicular tissues[11]. Nevertheless, the recent studies and applications showed that the extended setting time, potential of discoloration, low cell viability, and genotoxic elements (e.g., As, Ti, Al) in compositions have raised some concerns[12-14].

In this context, the desired features of filling materials should possess 1) good re-mineralization to facilitate sealing the root canal and promote the integration of materials and periapical tissues; 2) excellent osteogenesis and appropriate biodegradation to promote cementum/bone tissue regeneration; and 3) permanent

antibacterial property to inhibit bacteria growth in periapical area[15,16]. It is generally noted that silicon is essential to young bone growth and metabolism[17]. As an essential trace element in nutrition, silicon plays an important role in nucleation and growth of apatite, and influences the metabolism of osteoblast essential in the mineralization process and bone-bonding mechanism[18,19]. Moreover, the solutions of appropriate silicon concentration showed potential capacity to activate bone-related gene expression, stimulate osteoblast proliferation, and promote new bone tissue formation[20,21]. Some new materials such as antibacterial agent-loaded mesoporous Ca-silicate particles and related cements have recently been developed as root canal filling materials[22,23]. But the respective disadvantages such as lack of self-setting/hydraulicity and antibacterial properties would affect their applications in root canal therapy areas.

Recently, the hydraulic self-setting Ca-silicates have attracted great attention in orthopaedics and endodontics because of their good bioactivity and self-setting property[24-28]. β-C_2Si is known to react with water to form a sticky calcium-silicate-hydrate gel (so-called 'C-S-H') responsible for the continuing development of mechanical strength in Portland cement. Our and other's studies have showed that β-C_2Si is bioactive, through the development of an apatite mineral layer in biological fluids[28,29] and supports osteogenic cell and dental pulp cell growth[30,31]. Moreover, the formation rate of apatite on β-C_2Si is faster than that of other calcium-based biomaterials[32], which plays an important role on the formation of neonatal dentin and dentin bridge[33]. Of note, relatively high reactivity is desirable but the production of free CaO must be avoided due to its influence on setting rate of pure β-C_2Si. On the contrary, the CaO byproduct in β-C_2Si synthesis provides the opportunity to develop a long-term antibacterial filler to meet some challenging criteria in endodontics.

This study is aimed to develop a new adjustable free CaO, β-C_2Si-based cement by adding α-calcium sulfate hemihydrate (α-CSH) for endodontic use as alternative to MTA. It is known that α-CSH can rapidly react with water to form hydraulic calcium sulfate dihydrate (CSD, so-called gypsum) cement. The gypsum has enjoyed a longer history of clinical use for bone augmentation because of its fast self-setting property, good biocompatibility, and a rapid bioresorption in vivo[34]. In this study, the choice of the two components in the CaO-rich C_2Si/CSH composite system is based on the function-integrating concern that the hydration of α-CSH is extremely fast (tens of minutes) so that gypsum is mainly responsible for the initial cement setting and mechanical strength, while C-S-H contributes to the later hardens (i.e. long-term sealability) and continued antibacterial and bioactive properties. In this regard, the self-setting properties of the C_2Si/CSH system may be easily adjusted by α-CSH. Thus, the effects of free CaO and α-CSH contents on the physicochemical properties of the composites were systematically studied, and their bioactivity, antibacterial activity and antimicroleakage performance in root canal ex vivo were also evaluated.

Materials and methods

Powder preparation

The reagent-grade chemicals were bought from Sinopharm Reagent Co., Shanghai and used directly. The nominal β-C_2Si powders with different Ca/Si molar ratio (thereby signed as β-C_xSi; x=2.0, 1.8, 1.6, 1.4) in the reaction system were prepared by a sol-gel method[28]. According to the solution parameters shown in Table 1, calcium nitrate, tertraethyl orthosilicate (TEOS), and acetic acid were added to ethanol-water mixture under magnetic stirring. The sol was aged at 60°C for 48 h, dried at 95°C for 8 h, and calcined at 800°C for 2 h. The β-C_xSi powders were milled to 2–17 μm in particle sizes, and the free CaO (f_{CaO}) were determined by a glycol–ethanol method[35].

The α-CSH powder were prepared via a phase transformation process by low thermal treatment of a mixture solution containing 15% CSD, 15% NaCl, and 0.12% citric acid at 99°C for 5 h under stirring. The powders were characterized by X-ray diffraction (XRD; Rigaku) and scanning electron microscope (SEM; HITACHI, S4800). The pH values of β-C_xSi powder suspension in PBS (1.0 g/10 ml) were firstly measured by using a pH meter (Hanna Instruments, pH211) at different time intervals.

Table 1. Solution conditions and the products with different free CaO.

Sample	$Ca(NO_3)_2 \cdot 4H_2O$ (g)	C_2H_5OH (ml)	TEOS (ml)	acetic acid (ml)	water (ml)	free CaO
$C_{2.0}Si$	119.27	309.7	55.8	0.5	27	12.32%
$C_{1.8}Si$	119.27	310.7	61.3	0.5	30	4.76%
$C_{1.6}Si$	119.27	312.6	72.5	0.5	35	3.04%
$C_{1.4}Si$	119.27	314.6	83.6	0.5	45	1.41%

Paste preparation

The initial solid phase was prepared by manually mixing β-C_xSi and α-CSH powders with different CSH content (y%). The mixed powders were each weighted to obtain 20 g of cement powder, hereinafter referred as C_xSi/CSHy (x=2.0, 1.4; y=0, 10, 20, 30), and then ground for 10 min in a planetary ball mill for better homogeneity. The mixtures were then sterilized by dry heating in a stove at 120°C for 25 min, and followed by moistening by deionized water with a liquid-to-powder (L/P) ratio of 0.6 ml g^{-1}. The pastes were stirred for 30 s, transferred to stainless steel molds with a diameter (Ø) of 6.0 mm and stored in a 100% humidity water bath at 37°C.

Mechanical strength analysis

Compressive strength and three-point bending strength of the cement samples (Ø 6×9 mm; 35×8×6 mm) was measured at a loading rate of 1 mm min^{-1} with a universal testing machine (Instron, USA) until failure. The cements with L/P=0.6 were firstly stored in 100% humidity at 37°C for given interval (1, 3 and 28 d) and then used for mechanical strength testing.

Injectability

The injectability of $C_{2.0}Si$/CSHy (y=0, 10, 20, 30) pastes was estimated from the mass percentage of cement paste that could be injected using an 8.5 mm inner diameter, 5 ml syringe, with two types of needle of 21G (Ø 0.51 mm) and 16G guage size (Ø 1.19 mm)[36]. Typically, 5.0 g of paste was prepared, loaded into the syringe and mechanically injected at a constant pressure of 6.8 bar. Injection was repeated for different times until the paste was no longer completely injectable. Also, the injectability of $C_{2.0}Si$/CSHy (y=70, 80, 90, 100) paste was tested while other conditions remained same. The mass of transferred paste and the

mass remaining in the syringe were weighed and the percentage calculated against time.

Setting time

Initial (I) and final (F) setting times were measured with the Vicat needle according to ISO9597-1989E[30]. The initial setting time *I* is defined as the time necessary so that the light needle (280 g, diameter 1.13 mm) plunges into the paste and has a span of 5±1 mm to the tube bottom. The final setting time *F* is defined as the time necessary so that heavy needle (350 g, diameter 2.0 mm) no longer leaves a visible print on the surface of the paste.

Degradation and pH variation in vitro

Degradation behavior of the 4-h-set $C_xSi/CSHy$ cement (Ø8.0 mm ×4 mm) was estimated in 0.05 mol l^{-1} Tris buffer (pH 7.4) at 37°C with a surface area-to-volume ratio of 0.1 cm^{-1}. A quarter of the aqueous buffer was refreshed every day. At the preset time point, the pH variation of the cement bed by contacting the electrode head during immersion was measured as the method reported previously[37]. pH=f(t) plots were recorded with different f_{CaO}. Then, the cement samples were removed from the buffer, gently rinsed with absolute ethanol, and dried (75°C) up to mass constancy before weighing. The weight loss (degradation) was expressed as the percentage of the initial weight.

Bioactivity in vitro

The simulated body fluid (SBF), with ion concentration nearly equal to that of human blood plasma was prepared according to the Kokubo's recipes[38]. The human freshly extracted teeth with mature apices and single canal configuration were obtained from Hangzhou Dental Hospital. The teeth were cut to expose the apical root canal. For characterization of apatite-mineralization ability in vitro, the fresh paste was injected into the 6 mm-long root apex and stored in 100% humidity for 48 h and then immersed in SBF at 37°C with cement mass to SBF volume ratio of 1.0 mg ml^{-1} for 72 h. At the preset time point the pH value was measured and then, 2 ml of supernatant was refreshed with fresh SBF for ion concentration measurement by inductively coupled plasma (ICP). The specimen was gently rinsed with ethanol and dried in vacuum overnight for SEM observation.

Endodontic space sealing ex vivo

Human freshly extracted teeth free of crack, single-rooted, were used in this study. External calculus and tissue debris were carefully removed with a scalpel blade. Each root canal was drilled to the apical foramen with sequential files beginning with size 15. The teeth were radiographed to confirm the extension of straight canals and were decoronated to a standardized root length of 14 mm from apex. The teeth were divided into six groups of 6 canals, each group being filled with one of the $C_xSi/CSHy$ (*x*=2.0, 1.4; *y*=0, 10, 30) paste. All groups were kept in 100% humidity at 37°C for 48 h and they were again covered with a new layer of nail varnish leaving only the apex (~1 mm) free for penetration in order to assess the degree of infiltration in coronal-apical direction. Three teeth without filler were also sealed externally with nail vanish as positive control. The specimens were stored in air at room temperature for 12 h and then immersed in 0.5% Rhodamine B at 37°C for 72 h, using vacuum in the first 10 min. To highlight the dye penetration, cross-sections were made longitudinally with a low speed carborundum disk.

Antibacterial activity in vitro

Direct antimicrobial activity of the cements was tested by agar diffusion using actinomyces viscosus (*A.viscosus*), actinomyces naeslundii (*A. Naeslundii*), and streptococci mutans (*S. mutans*). The cement discs (Ø 8 mm×2 mm; *n*=6) were prepared at a peak loading rate of 2.5 g cm^{-2} using Teflon model. The cement discs were allowed to set at 37°C and 100% humidity for 24 h. The bacterial strains were maintained as subcultures on trypticase soy agar (TSA) plates at 37°C in an anaerobic chamber, where O_2 and H_2 were purged down to 100 ppm and 1%, respectively, using N_2 and biological atmosphere mixture (5% CO_2 in N_2). The preset cements were placed at the centre of the agar plate and the inhibition zone around the cements were quantified using a 0.5-mm-precision rule after incubation for 24 h.

Statistical analysis

Experimental results were expressed as means ±SD. Statistical analysis was carried out using one-way ANOVA, and a *p*-value of less than 0.05 was considered statistically significant.

Results and discussion

Physicochemical characterization of the powders

Figure 1 shows the XRD patterns of β-C_xSi (*x*=2.0, 1.8, 1.6, 1.4) powders with different Ca/Si molar ratio in the beginning sol medium. Comparison with the standard XRD pattern of β-C_2Si (JCPDS 33-0302), it is clear that the sol-gel-derived powder was mainly composed of β-C_2Si, and CaO was also observed. The peak intensity (37.36°, 53.84°/2θ) for CaO tended to increase with the increase of Ca/Si molar ratio in the beginning sol, which was consistent with the quantitative results (f_{CaO}; Tab. 1). However, our previous study showed that the colloidal SiO_2 and $Ca(NO_3)_2.4H_2O$ with an initial Ca/Si molar ratio of 2.0 as starting materials could produce very pure β-C_2Si[28]. These differences were possibly attributed to the rapid hydrolysis and condensation reactions of TEOS by acid catalysis to form silica gel, which resulted in the increase of free CaO in the products. As for the particle morphology, the SEM images (Fig. 1, inset) indicated that the powder samples had particle-like shape with heavily

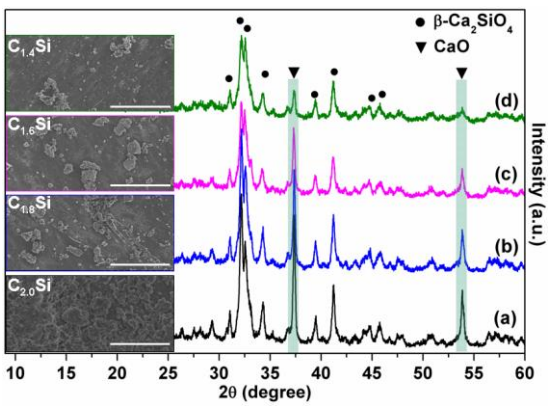

Figure 1. XRD patterns of β-C_xSi powders. Inset representing the SEM images of the powders (Bar: 50 μm).

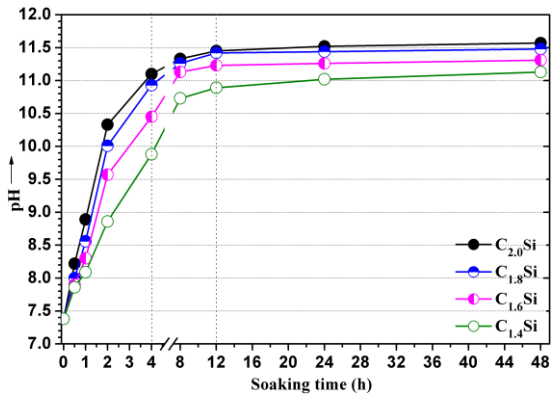

Figure 2. Changes in pH value of PBS medium during immersing the β-C_xSi powders (100 mg/50 ml).

agglomerative morphologies, and the particle size was below 20 μm. As for the α-CSH, it showed polyhedra crystals with size of 10−20 μm (see Fig. S1; Supporting Information (SI)).

The pH value of the immersion medium inside the β-C_xSi suspension increased markedly from the initial value of 7.4 immediately (Fig. 2). Although the values varied depending on the powder composition, similar trends in pH change were observed for all samples. The greatest rate of pH increase was recorded within 1−2 h, and the maximum level was achieved at 8−12 h, and thereafter kept stable. Moreover, the higher pH was seen with the powders of β-$C_{2.0}Si$ and β-$C_{1.8}Si$ than with the powders of β-$C_{1.6}Si$ and β-$C_{1.4}Si$. Obviously, β-C_2Si and free CaO were the two essential ingredients responsible for the development of the "early" and "late" pH value increase due to their different reactivity in water. When contact with water, the powders reacted with water to form calcium silicate hydrates (C-S-H) and CH according to the reactions as following:

$$CaO+H_2O \rightarrow Ca(OH)_2 \quad (1)$$

$$2Ca_2SiO_4+4H_2O \rightarrow 3CaO{\cdot}2SiO_2\ 3H_2O+Ca(OH)_2 \quad (2)$$

Microstructure, mechanical development of the pastes

It can be seen that the pure α-CSH in contact with water quickly transformed to fiber-like gypsum cement at 24 h (Fig. S2; SI). However, the so-called C-S-H in the cross-sectional superstructure of $C_xSi/CSHy$ composites grew as interlocking aggregates within 3 d and especially the fiber-like CSD could be seen in the CSH-rich $C_{1.4}Si$/CSH30 cement (Fig. 3).

It is worth noting that the content of free CaO and α-CSH component heavily influence the strain of composite cements. As shown in Figure 4a, the low CaO content and high α-CSH component were both favorable for improving compressive strength. The values for the $C_{2.0}Si$/CSH0 and $C_{2.0}Si$/CSH10 after setting for 3 d were 10.9±0.5 and 14.7±0.8 MPa, respectively, indicating significant difference (p<0.05). Moreover, the strength development of the hydraulic pastes also indicated a mild increase with prolonging setting time because the hydration rate of β-C_2Si was much slower than α-CSH, and thus storing the composite cements in a wet environment gave it more compressive strength with the passage of time. In the case of $C_{2.0}Si$/CSH10, for instance, the setting time (3 d and 28 d) significantly (p<0.05) affected the compressive strength (14.7±0.8 Mpa; 19.5±1.2 MPa) of the cements. Similarly, the

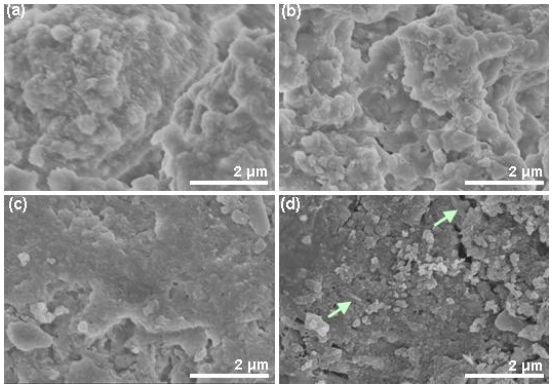

Figure 3. SEM images of the $C_{2.0}Si$/CSH10 (a) $C_{2.0}Si$/CSH30 (b), $C_{1.4}Si$/CSH10 (c) and $C_{1.4}Si$/CSH30 (d) cements after curing for 3 d. The arrow showing the needle-like CSD crystals.

bending strength showed a slight increase with addition of α-CSH component and a prolongation of setting time from 1 to 3 d (Fig. 4b), but this strength was significantly lower than the compressive strength of the samples set under same conditions.

It is known that when the β-C_2Si or β-C_3Si powders and water are mixed in an appropriate ratio, they form a paste that hardens by entanglement of the crystal precipitated in the paste. Chang's group have found that there existed as a mass of interlocking C-S-H needles in the cross-section of pure β-C_2Si or C_3Si cement [30,39], but such superstructure were not observed in the CSH-added C_3S composite cements. It is reasonable to postulate that the dissolved SO_4^{2-} groups from gypsum in the $C_xSi/CSHy$ cements may interfere in the oriented growth of C-S-H phase, so that the gypsum would partly contribute to the strength development of the hydraulic composite cements.

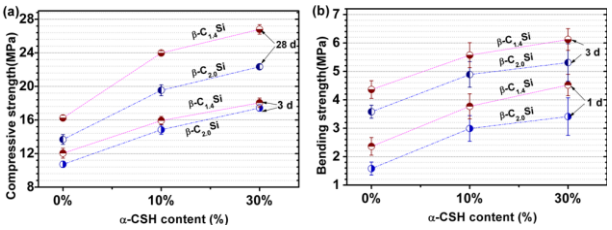

Figure 4. Mechanical strengths of the $C_xSi/CSHy$ cements with different α-CSH contents after setting for different time stages curing in 37°C and 100% relative humidity.

Injectability and setting time of the pastes

The paste injectability and setting time are both clinically relevant factors in root canal treatment. Composition of powders, particle size, liquid phase, and the *L*/*P* ratio, play crucial roles in the setting time and injectability[40]. Our experiments were performed to evaluate the influence of CSH content on the β-$C_{2.0}Si$-based cement setting. The results (Tab. S1; SI) indicated that the CSH content greatly affected the setting time. A decrease in setting time was observed with the increase of the CSH content. Increasing CSH content from 0% to 30% resulted in a clear decrease in *I* from 38 to 22 min and *F* from 65 to 26 min.

Usually, guage sizes of G10–16 would be useful for orthopedic procedure, whereas G16–25 would be suitable for dental applications[38]. In this study, all composite cements consisting of a limited mass percent (≤30%) of α-CSH in the primary powders

could be injected over 90% of the paste through the 16G needle within 8 min (Fig. 5a), yet only 3 min for the 21G needle (Not shown). With increasing α-CSH content up to 70%, their injectability deteriorated rapidly. Figure 5b−d shows that the β-$C_{2.0}Si$, $C_{2.0}Si$/CSH10 and $C_{2.0}Si$/CSH30 may form continuous linear pastes from the larger and smaller nozzle, respectively, while pure α-CSH paste shows poor injectability with inhomogenous paste under the same condition (Fig. 5e). These results imply that the injectable time of C_xSi/CSH*y* ($y \leq 30\%$) is advantegeous for canal filling treatment. On the other hand, the high content of free CaO in β-$C_{2.0}Si$ powder (as antibacterial agent in the present study) can be assumed to increase interfacial energy and retard the hydration and hardening reaction of β-$C_{2.0}Si$-based powders[41]. This means that addition of appropriate amount of α-CSH is favorable to improve the workability and accelerate hydraulic reaction.

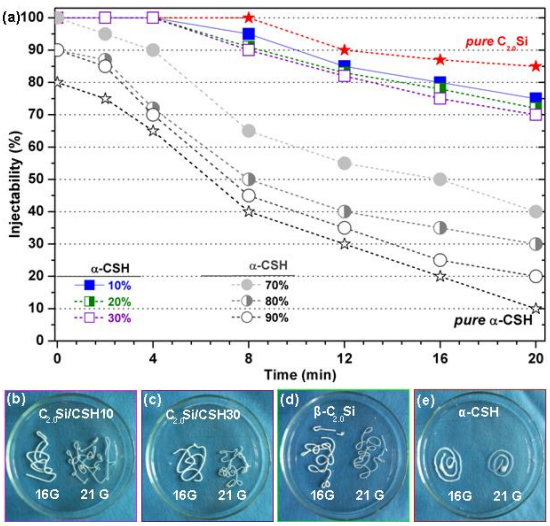

Figure 5. Injectability of the $C_{2.0}Si$/CSH*y* composite pastes at *L*/*S* ratio of 0.60 ml/g (a) and outward appearance of the injected paste of $C_{2.0}Si$/CSH10 (b), $C_{2.0}Si$/CSH30 (c), pure β-$C_{2.0}Si$ (d), and pure α-CSH (e) after injecting from two types of needle nozzles (16 G and 21 G).

Biodegradation and pH change in immersion medium

Conventionally, insolubility and low solubility is a characteristic of root-end filler that is of utmost importance and necessary for successful results. On the other hand, the gypsum content is a key parameter controlling the biodegradation ratio of the gypsum-containing composite cements in vitro and in vivo[42]. As shown in Fig. 6a, the degradation of the current β-C_2Si-based cements was a slow process, and the degree of degradation was time and CSH content dependent. It is evident that the weight loss may be because of the release of soluble fractions (mainly CSD and CH) in the β-$C_{2.0}Si$- and β-$C_{1.4}Si$-based cements. In terms of CSH content, the cement weight of β-$C_{2.0}Si$, $C_{2.0}Si$/CSH10 and $C_{2.0}Si$/CSH30 reduced to 8.1%, 9.4% and 11.3% after 48 h of soaking, respectively; afterwards, the pure β-$C_{2.0}Si$ showed ~83% material residue on day 28, in contrast with those (~76%) for the composite cements containing 10−30% α-CSH. This means that addition of α-CSH leads to accelerate biodegradation of the composite cements.

Figure 6b presents the time-dependent pH changes of the cement-immersed media. It is clear that the higher was CaO content in the primary powders, the greater rate of pH increase was recorded in the paste bed. The pH values in all solutions increased quickly from the initial value of 7.4 to 8.0−8.4 at 2 h, mainly due to the release of CH from cement. In particular, the pH values strongly increased in the β-$C_{2.0}Si$-based cement bed within 48 h; this was not the case for the β-$C_{1.4}Si$-based cements. Although the Tris buffer was partly refreshed every 24 h, the pH increased mildly with prolonging time possibly due to the production of CH byproduct during hydration of β-C_2Si as the reaction (2) above. In particular, the maximum level of pH value (~10.9) was seen with the β-$C_{2.0}Si$-based cements than that (~9.4) with the β-$C_{1.4}Si$-based cements. These results suggest that the pH value in the cement bed is companied with a two-step increase: in the first, a combination reaction of free CaO occurs quickly, producing CH and releasing hydroxide ion (OH^-); in the second, the β-C_xSi reacts with water to produce C-S-H and CH byproduct. β-C_xSi reacts slower than CaO with water, and then predominantly participate in the long-term pH maintainance. These "early" and "late" reactions are of high benefit for the antibacterial requirement in canal sealing treatment.

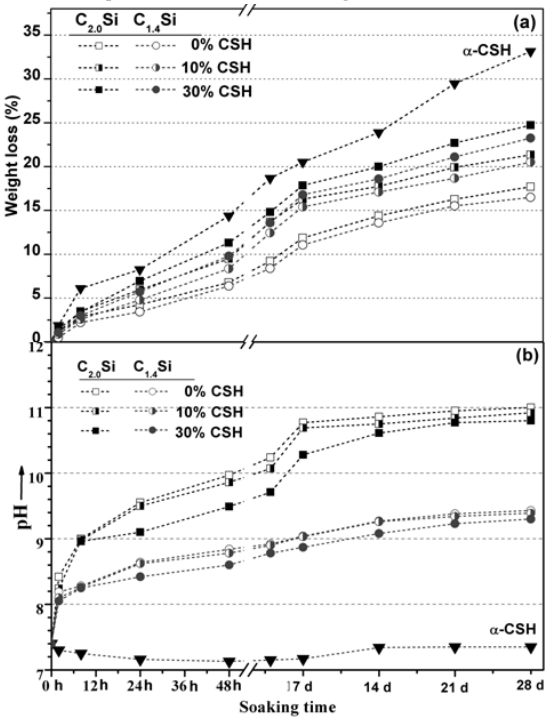

Figure 6. Weight loss of the cements (a) and changes in pH value (b) during soaking in 50 mM Tris.

Apatite-mineralization and sealability of the cements

Another significant advantage for the β-C_2Si-based cements is its excellent bioactivity (i.e. apatite-mineralization) in (simulated) biological solution. It is well agreed from the widespread studies that apatite-mineralization of biomaterials benefits the integration with host bone tissue[43], and especially the deposited biomimetic apatite on the artificial biomaterials possesses the capacity to enhance osteogenic cell activity, including proliferation and differentiation[44]. In this study, it is found that the β-$C_{2.0}Si$ and C_xSi/CSH*y* composite pastes easily filled in the apical root canal cavity (Fig. 7a–d). In particular, the cements all formed bond tightly with the cave wall of the root canal of teeth, without any

defect in the interface zone between cement and tooth after setting for 48 h. After soaking the cement-filled apical canal of a tooth in SBF for 72 h, new apatite-like crystal clusters that were several microns in size and spindle morphology were formed on the surface of the cements (Fig. 7e–h). The deposition layers on pure β-$C_{2.0}$Si and the composite cements were similar in morphology, and the EDX analysis revealed that there were P element in the EDX spectrum and the ratio of Ca/P for the formed apatite was 1.57~1.62, in contrast with only Ca, Si and S elements for cements before soaking in SBF (Not shown). In addition, the weak basic paste led to pH increase (Fig. S3; SI) and rapid release of Ca^{2+} ions (Fig. S4; SI) in SBF within 24 h. However, the P concentration began to decrease at 16 h and the increase of Ca concentration was very slow after 24 h, implying apatite or its precursor readily deposit on the exposed cement surface. These results suggest that the composite cements possess good apatite-mineralization ability in the apical root canal cavities of teeth.

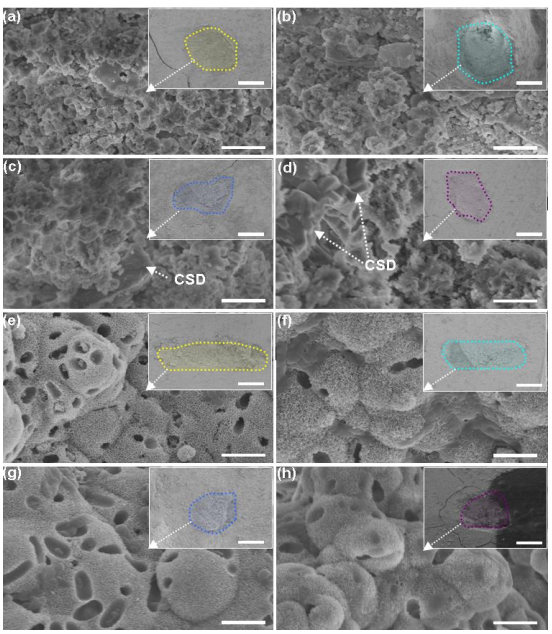

Figure 7. High magnification SEM images showing the cements before (a–d) and after (e–h) soaking in SBF for 72 h (Bar: 2 μm). Inset (low magnification SEM image; bar: 500 μm) showing the apex root of a tooth filled with the cement (dot-line circles). (a, e) β-$C_{2.0}$Si, (b, f) $C_{2.0}$Si/CSH10, (c, g) $C_{2.0}$Si/CSH30, (d, h) $C_{1.4}$Si/CSH30.

The ex vivo apical microleakage was tested in dye solution, as shown in Figure 8a. According to the optical microscope observation, the microleakage distance of the filling cements was slightly increased when the α-CSH content was increased in the initial powder composites. As can be seen in Fig. 8b, all of the longitudinally sectioned root canal fillers with C_xSi/CSH*y* had good adaptation to the canal wall, without forming gaps or voids in the interface zone, afforded tighter adaptation to the dentin. Although there was no significant difference in adaptation to the root canal wall between the pure β-C_2Si cement and that containing 10% of α-CSH, the cements in the absence and presence of α-CSH exhibited some different degree of dye penetration. It was seen from Fig. 8c that Rhodamine B penetration distance into pure β-$C_{2.0}$Si and β-$C_{1.4}$Si cements ranged from a minimum of 1.0 mm to a maximum of 1.5 mm, with a mean value of 1.1 mm and 1.3 mm, respectively. The microleakage distances of the C_xSi/CSH*y* (x=2.0, 1.4; *y*=10, 30) filling cements were in the range of 1.6~2.0 mm, indicating a significant difference (p<0.05) between the composites with 30% CSH and pure β-C_2Si alone. It implies that more CSH dissolution into medium leads to a reduction in anti-microleakage.

Antibacterial properties of composite cements

The C_xSi/CSH-*y*% (*x*=2.0; *y*=0, 10) formulations inhibited growth of *S. mutans*, *A. naeslundii*, and *A. viscosus*, as clear rings appearred around cement samples inserted into the agar plate. The β-$C_{2.0}$Si markedly inhibited the growth of *A. viscosus*, producing a large zone of inhibition observed in this study (Fig. 9a−f). In particular, the β-$C_{1.4}$Si-based composite cements appeared to cause much smaller inhibition zones than the β-$C_{2.0}$Si-based cements containing high CaO content; for instance, the $C_{1.4}$Si/CSH10 had no substantial effect on the bacterial viability (Fig. 9g). Moreover, the more CSH was present in the composite cements, the higher was survival of the bacteria in the culture system. These results suggest that a high level of free CaO and a small level of CSH introduction in β-$C_{2.0}$S have a considerable effect on inhibiting the oral microbia viability.

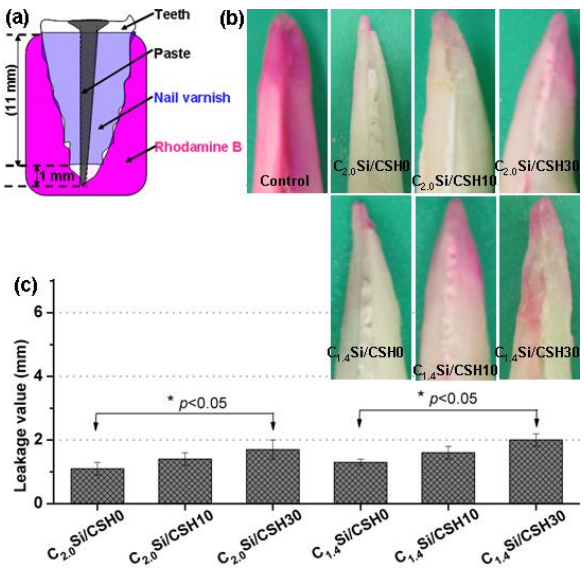

Figure 8. Schematic leakage model (a), leakage pattern according to cement composition (b), and dye leakage values of the cement fillers (c).

It is known that MTA-based root-end filling is a promising therapeutic approach for root perforation repairs and pulpal capping. However, the release of arsenic from MTA have been raised a matter of concern[10]. Most recently, Silva and co-workers[14] investigated the effect of root canal sealer on the cytotoxicity of fibroblast for a period of 5 weeks. They found that the fresh MTA exhibited severe toxicity initially and remained moderately toxicity after end of the experimental period. Meanwhile, the elute of MTA in simulated body fluid presented varying degrees of cytotoxcity. This long-term evaluation is more advantageous than previous strategies that assessed cytotoxicity for a shorter period because it enables establishing the preculiar toxicity profiles of that are characteristic of specific sealer. Therefore, it is critical to develop novel strategies for improving biocompatibility and endowing multiple functions to achieve a

synergistic therapy under a variety of clinical conditions. The present study summarizes our effort to prepare highly bioactive filling cements based on a new established β-C_2Si-based composition. In order to achieve this objective, the rapid setting α-CSH is used for the preparation of the β-C_2Si-based composites with the aim of guaranteeing excellent bioactivity and appropriate biodegradability, without compromising its sealability and biological properties. It is well accepted that when implanted alone at extraskeletal or root canal sites, the gypsum-based cements undergoes rapid biodissolution with limited new hard tissue formation or mineralization[35,42]. This is obvious to affect the sealing ability of the hydraulic sealer in root canal environment. Therefore, addition of a limited amount of CSH (e.g. 10 wt%) into the β-C_2Si powder in this study, the composite paste shows good antimicrobial and anti-microleakage properties.

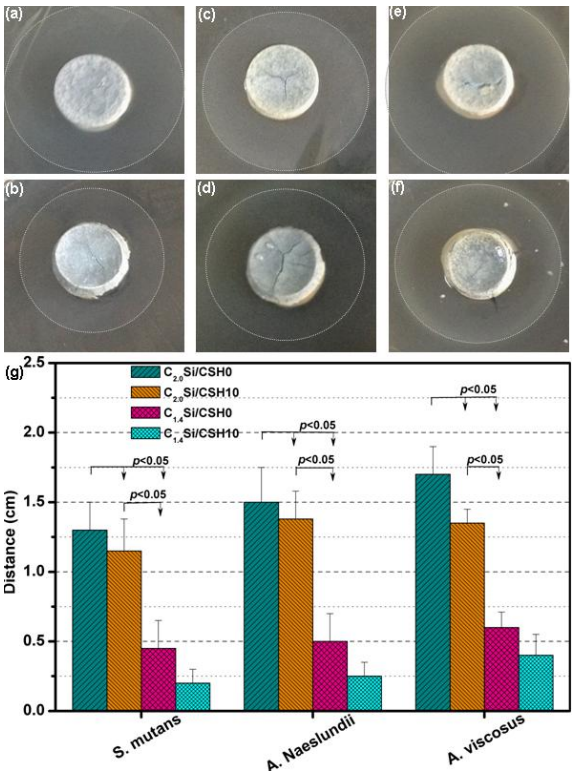

Figure 9. Agar diffusion test of the pure $C_{2.0}$Si (a, c, e) and $C_{2.0}$Si/CSH10 (b, d, f) formulation with *S. mutans* (a, b), *A. naeslundii* (c, d), *A.viscosus* (e, f) bacterial stains. (g) Quantitative results (diameter) of the zone of bacterial growth inhibition against of the *S. mutans*, *A. naeslundii*, and *A.viscosus* bacterial strains in presence of C_xSi/CSH*y* (*x*=2.0, 1.4; *y*=0, 10).

It is widely reported that the antibacterial activity of Ca-silicate bioglass is mainly based on several factors, including high pH and osmotic effects caused by non-physiological concentration of ions dissolved from the materials[45-47]. CH-containing pastes can be used as intracanal medication due to the high aqueous pH value caused by CH dissolution. However, Jainaen et al. reported that the CH paste pH 12.5 may kill *S. mutans*, *A. viscosus*, and *S. aureus* within 6 h, whereas the paste pH below 10 could not kill any bacteria[48]. This suggests that the antibacterial effect is not always fully achieved in clinical practice if the amount of CH in the permanent filling paste is limited. Ding is one of the pioneers in developing the Ca-silicate cements (i.e. calcium silicate/dicalcium silicate composite) as potential sealer for endodontic treatment[25,32,49], whereas their quick-setting material systems with low Ca/Si molar ratio (≤1.6) contain limited CaO (equivalent to that in $C_{1.6}$Si or $C_{1.4}$Si in this study) and thus the antibacterial activity would be extremely limited. In the present study, the CaO-rich β-C_2Si-based cements (e.g. $C_{2.0}$Si/ CSH10) are revealed to show a growth inhibition of the typical oral microorganisms causing e.g., pulpal necrosis and periapical lesions. Our results demonstrate that the level of pH value of root-end filling materials is critical to its antibacterial activity.

It should be emphasized that the method of solubility assessment in most studies, including ours in the present study, is based on the difference between weight before and after placing the Ca-silicate cements into the water[50,51]. Although it is a standard method for assessing material solubility, the test, in fact, measures the elution of water-soluble material, not the solubility. Thus the early-stage weight loss for the C_xSi/CSH*y* system can be mainly attributed to the dissolution of CSD component. On the other hand, although the surface porosity on the set C_xSi/CSH composites is maybe a potential drawback for the cements, it is remarkable that a layer of apatite remineralize over the material that may fill the surface voids and even significantly attenuates or completely reverses CSH-induced biodissolution. The apatite-mineralization is a very desirable phenomenon in root canal filling therapy because this phenomenon increases the sealing ability of filling materials and promotes regeneration of the original tissues when it is placed in contact with the dental pulp or periradicular tissues[52]. Consequently, the excellent apatite mineralization potential of the C_xSi/CSH*y* cement is of high benefit to improve chemical bonding between the material and the dentinal and the detrimental effects due to biodissolution and potential microleakage can be avoided. Meanwhile, this also might be the key characteristic responsible for the successful performance in promoting apexification for a large open apical foraminal with more new bone and cementum formation in comparison with other conventional filling material systems.

Conclusion

In summary, we demonstrated the advantageous combination of physicochemical properties and antibacterial performance of β-C_2Si and α-CSH and a bioactive and long-time antibacterial root filling biocement is developed. The controllable free CaO in the β-C_2Si products could adjust the antibacterial levels, and a small level of α-CSH introduction in β-C_2Si has a considerable effect on the workability, strength development and injectable control, which is a clear advantage, as the long setting process is no longer critical for the formation of hydraulic cement compared to the CaO-rich β-C_2Si. The overall results suggest that the β-C_2Si promotes the apatite mineralization, and the apatite layer is found to be compact, continuous, and composed of many small crystallites, which would contribute to the quick bonding of the material to the dental pulp or periradicular tissues. Because of its simple composition characteristic (free of any genotoxic elements), good bioactivity, reasonable degradability, excellent sealing and antimicrobial properties, the C_2Si/CSH systems meet some challenging criteria in root canal sealing, especially in the capping of dental pulp tissues, root end closure, repair of root perforations as well as root end filling material to promote regeneration of original tissue when placed in direct contact with

periradicular tissues.

Acknowledgements

This work is supported by Hangzhou Science and Technology Bureau Foundation (20120633B19), Health Bureau of Zhejiang Province (2013KYA108), National Science Foundation of China (81271956, 51102211, 81301326), the Fundamental Research Funds for the Central University (2012QN81001), and Yiwu Science and Technology Bureau Foundation (No. 120315).

Notes and references

[a] *Zhejiang-California International Nanosystems Institute, Zhejiang University, Hangzhou 310058, China. Fax: 86-571 8697 1539; Tel: 86-571 8820 8353; E-mail: zhrgou@zju.edu.cn*

[b] *Hangzhou Dental Hospital. Pinghai Road No.57, Hangzhou 310020, China. Fax: 86-571 8708 8567; Tel: 86-571 8708 8567; E-mail: iamliumin@126.com*

[c] *The First Affiliated Hospital, College of Medicine of Zhejiang University, Hangzhou 310003,China*

[d] *Department of Stomatology Children's Hospital School of Medicine, Zhejiang University, Hangzhou 310006, China*

† Co-first author.

1. D. R. Nixdorf, A. S. Law, J. O. Look, D. B. Rindal, E. U. Durand, W. Kang, B. S. Agee, J. L. Fellows, V. V. Gordan and G. H. Gilbert, J Endod. 2012, **38**, 1470–8.
2. L. A. da Silva, M. R. Leonardo, R. S. Silva, S. Assed and L. F. Guimaraes, Int Endod J. 1997, **30**, 205–9.
3. L. Hammarstrom, L. B. Blomlof, B. Feiglin and S. F. Lindskog, Endod Dent Traumatol. 1986, **2**, 184–9.
4. M. Trope, J. Moshonov, R. Nissan, P. Buxt and C. Yesilsoy, Endod Dent Traumatol. 1995, **11**, 124–8.
5. L. K. Bakland and J. O. Andreasen, Dent Traumatol. 2012, **28**, 25–32.
6. P. Saxena, S. K. Gupta and V. Newaskar, Restor Dent Endod. 2013, **38**, 119–27.
7. T. H. Huang, S. J. Ding and C. T. Kao**,** J Biomed Mater Res B. Appl Biomater. 2005, **80B**, 486–90.
8. M. Parirokh and M. Torabinejad, J Endod. 2010, **36**, 16–27.
9. M. Parirokh and M. Torabinejad, J Endod. 2010, **36**, 190–202.
10. M. Parirokh and M. Torabinejad, J Endod. 2010, **36**, 400–13.
11. M. Torabinejad and N. Chivian, J Endod. 1999, **25**, 197–205.
12. C. Estrela, P. F. Estrada-Bernabé, D. de Almeida-Decurcio, J. Almeida-Silva, C. Rodrigues-Araújo-Estrela and J. A. Poli-Figueiredo, Med Oral Patol Oral Cir Bucal. 2011, **16**, e418–24.
13. C. S. Ribeiro, M. F. Scelza, R. Hirata Júnior and L. M. Buarque de Oliveira, Oral Surg Oral Med Oral Pathol Oral Radiol Endod. 2010, **109**, e109–12.
14. E. J. Silva, C. C. Santos and A. A. Zaia, J Appl Oral Sci. 2013, **21**, 43–7.
15. D. Ørstavik, Endod Topics, 2005, **12,** 25–38.
16. S.R. Priyanka and Dr.Veronica, IOSR J Dent Med Sci. 2013, **9**, 20–5.
17. K. Schwarz and D. B. Milne, Nature. 1972, **239**, 333–4.
18. C. Knabe, M. Stiller, G. Berger, Clin Oral Impl. Res. 2005, **16**, 119–26.
19. J. Sun, Jy. Li, Xy Liu, L. Wei, G. Wang and F. Meng, Biomed. Pharmacotherapy. 2009, **63**, 650–7.
20. J. Sun, L. Wei, X. Liu, J. Li, B. Li, G. Wang and F. Meng, Acta Biomater. 2009, **5**, 1284–93.
21. M.-Y. Shie, S.-J. Ding, and H.-C. Chang. Acta Biomater. 2011, **7**, 2604–14.
22. C. Wu, J. Chang and W. Fan, J Mater Chem. 2012, **22**, 16801–9.
23. H. K. Chng, I. Islam, A. U. J. Yap, Y. W. Tong and E. T. Koh, J Endod. 2005, **31**, 665–8.
24. M. G. Gandolfi, F. Perut, G. Ciapetti, R. Romano Mongiorgi and C. Prati, J Endod. 2008, **34**, 39–44.
25. C. C. Chen, C. C. Ho, C. H. Chen and S. J. Ding, J Endod. 2009, **35**, 1288–91.
26. R. Du, T. Wu, W. Liu, L. Li, L. Jiang, W. Peng, J. Chang and Y. Zhu, J Endod. 2013, **23**, 1023–9.
27. M. G. Gandolfi, F. Siboni, A. Polimeni, M. Bossù, F. Riccitiello, S. Rengo and C. Prati, Dent J. 2013, **1**, 41–60.
28. Z. Gou and J. Chang, J Eur Ceram Soc. 2004, **24**, 93–9.
29. X Liu, S Tao and C Ding, Biomaterials. 2002, **23**, 963–8.
30. Z. Gou, J. Chang, W. Zhai and J. Wang, J Biomed Mater Res B. Appl Biomater. 2005, **37B**, 244–51.
31. C. C. Chen, M. Y. Shie and S. J. Ding, Int Endodontic J. 2011, **44**, 836–42.
32. C. C. Chen, C. C. Ho, C. H. Chen, W. C. Wang and S. J. Ding, J Endod. 2009, **35**, 1554-1557.
33. P. N. De Aza, F. Guitian and S. De Aza, Biomaterials. 2000, **21**, 1735–1741.
34. M. V. Thomas and D. A. Puleo, J Biomed Mater Res. Part B. Appl Mater. 2009, **88**, 597–610.
35. F. M. Lea, 3rd ed. Chemical Publishing Co., New York, 1971, p. 108.
36. E. F. Burguera, H. H. Xu and L. Sun, J Biomed Mater Res Part B Appl Biomater. 2008, **84**, 493-502.
37. J. Nurit, J. Margerit, A. Terol and P. Boudeville, J Mater Sci Mater Med. 2002, **13**, 1007–14.
38. T. Kokubo and H. Takadama, Biomaterials. 2006, **27**, 2907–15.
39. W. Zhao, W. Zhai, Z. Wang, J. Wang, J. Chang, Biomaterials, 2005, **26**, 6113–21.
40. M. Bohner and G. Baroud, Biomaterials. 2005, **26**, 1553–63
41. K. Fuji and W. Kondo, J Am Ceram Soc. 1979, **62**, 161–7.
42. G. Yang, M. Lin, L. Zhang and Z. Gou, J Inorg Mater. 2013, **28**, 795–803.
43. L. C. Palmer, C. J. Newcomb, S. R. Kaltz, E. D. Spoerke and S. I. Stupp, Chem Rev. 2008, **108**, 4754–83.
44. S. Midha, T. B. Kim, W. van den Bergh, P. D. Lee, J. R. Jones and C. A. Mitchell, Acta Biomater. 2013, **9**, 9169–82.
45. P. Stoor, E. Söderling and J. I. Salonen, Acta Odontol Scand. 1998, **56**, 161–5.
46. O. Lepparanta, M. Vaahtio, T. Peltola, D. Zhang, L. Hupa, M. Hupa, H. Ylanen, J. I. Salonen, M. K. Viljanen and E. Eerola, J Mater Sci: Mater Med. 2008, **19**, 547-551.
47. D. Zhang, O. Leppäranta, E. Munukka, H. Ylänen, M. K. Viljanen, E. Eerola, M. Hupa and L. Hupa, J Biomed Mater Res. Part A. 2010, **93A**, 475–83.
48. A. Jainaen, M. Nawachinda and Ra. Serinirach, CU Dent J. 2002, **25**, 161–73.
49. M. Y. Shie, H. C. Chang and S. J. Ding, Int Endod. J. 2012, **45**, 337–45.
50. Z. Huan, J. Chang, X.-H. Huang, J Biomed Mater Res B. Appl Biomater. 2008, **87B**, 387–94.
51. Z. Huan, J. Chang, Acta Biomater. 2009, **5**, 1253–64.
52. Z. Dong, J. Chang, Y. Deng and A. Joiner. Aust Dent. J. 2011, **56**, 175–80.